

Magma chamber formation by dike accretion and crustal melting: 2D thermo-compositional model with emphasis on eruptions and implication for zircon records

O. E. Melnik^{1,2*}, I. S. Utkin¹, and I. N. Bindeman^{3]}

¹Institute of Mechanics, Moscow State University, Moscow, Russia

²Fersman Mineralogical Museum, Russian Academy of Sciences, Moscow, Russia

³Department of Earth Sciences, University of Oregon, USA

*Corresponding author: Oleg Melnik (melnik@imec.msu.ru)

Contents of this file

Text S1 to S2
Figures S1 to S8

Additional Supporting Information (Files uploaded separately)

Movies S1 shows evolution of temperature, melt and dike volume fractions and kinematics of Lagrangian particles during magma body formation and cooling for $Q = 0.25 \text{ m}^3/\text{s}$ and $W = 10 \text{ km}$.

Introduction

Supplementary materials contain Texts S1 and S2 that describes validation procedure for the numerical method and provides MatLab code for the benchmark solution for a single dike cooling with heat and mass transfer. Additional figures are described in the main text.

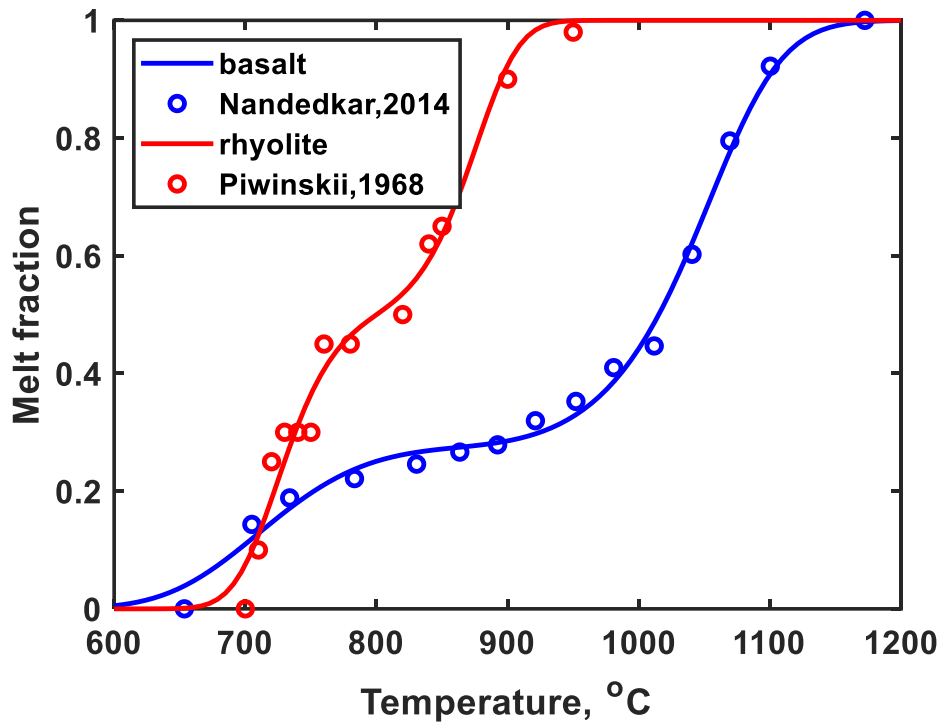


Figure S1. Phase diagrams used in the simulations.

Melt fraction as a function of temperature (in degC) is approximated as following:

Rhyolite:

```
function MF=mf_rhyolite(T)
```

```
    t2 = T .* T;
```

```
    t7 = exp(0.961e3 - 0.359e1 * T + 0.448e-2 * t2 - 0.187e-5 * t2 .* T);
```

```
    MF = 0.1e1 ./ (0.1e1 + t7);
```

```
end
```

Basalt:

```
function MF=mf_basalt(T)
```

```
    T=T/1000;
```

```
    a=143.6; b=-494.4; c=572.4; d=-221.4; t2 = T .* T;
```

```
    MF = 0.1e1 ./ (0.1e1 + exp(a + b .* T + c .* t2 + d .* t2 .* T));
```

```
end
```

Text S1. Numerical method validation.

We consider three benchmark studies to demonstrate validity and robustness of our numerical routines. In the first benchmark study heat conduction from a point source in an infinite domain is considered. We do not account for phase transitions in this problem, i.e., latent heat L is assumed to be equal to 0. An analytical solution of this problem exists in the form of a Green's function:

$$T_G(x, y, t) = \frac{T_a t_0}{t} \exp\left(-\frac{x^2 + y^2}{4\chi t}\right) \quad (S1)$$

which is a “hat-shaped” function for $t > 0$. Here, $t_0 > 0$ is some value of time, and T_a is an amplitude of temperature at $t = t_0$. For the purposes of numerical modeling, the finite domain $(x, y) \in [-l/2; l/2] \times [-l/2; l/2]$ is considered. To reduce the influence of boundaries, domain size l is chosen in such a way that the temperature $T_G(x, y, t)$ is close to zero at $x, y = \pm l/2$.

Results of numerical modeling are presented in Fig. S2. We assume that $\chi = 1 \text{ m}^2/\text{s}$ and $T_a = 1 \text{ K}$. As an initial condition, the analytical solution given by Eq. (S1) at $t = t_0 = 0.005 \text{ s}$ is used. Then, the simulation is advanced in time until $t = 0.01 \text{ s}$. This corresponds to 800 explicit time steps with grid spacing $\delta x = 0.005 \text{ m}$. As can be seen from Fig. S2, exact and numerical profiles for the temperature at $x > 0$ and $y = 0$ are in the good agreement.

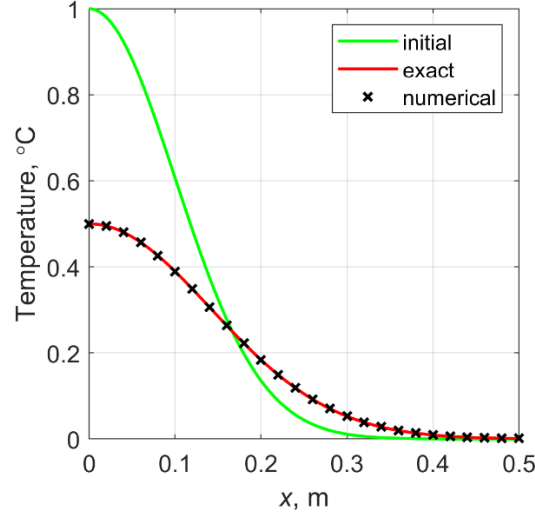


Figure S2. Comparison of the numerical solution to the heat diffusion problem and the analytical Green’s function. Curves and crosses are the profiles of temperature T at $x > 0$ and $y = 0$.

In the second benchmark study, cooling and solidification of an individual elliptical dike at different grid resolutions is considered. For comparison, we implemented a reference solver in Matlab language using the frequently employed enthalpy method. Complete listing of the reference solver is provided in this Supplementary material. Enthalpy formulation to the problem of heat conduction is as follows:

$$\frac{\partial H}{\partial t} = \nabla \cdot k \nabla T, \quad H(T) = \rho(cT + L\beta(T)) \quad (\text{S2})$$

where H is the enthalpy, T is the temperature, k is the thermal conductivity, ρ is the density, c is the specific heat capacity, L is the latent heat, β is the melt fraction.

To determine the temperature T , the dependence of H on T is tabulated, and the resulting table of H - T pairs is used to lookup the reverse relation $T(H)$. This is possible because $H(T)$ is a monotonous function.

Problem statement and initial distribution of temperature is shown in Fig. S3a. We consider a rhyolitic dike with half-length $a = 1350 \text{ m}$ and half-width $b = 10 \text{ m}$. The initial temperature at time $t = 0$ in the dike is $900 \text{ }^\circ\text{C}$, and the initial temperature in surrounding rocks is $500 \text{ }^\circ\text{C}$. Heat transfer between dike and rocks over $t_{tot} = 500 \text{ y}$ is modeled using both reference Matlab solver and CUDA GPU code. The reference simulation is carried out with grid spacing $\delta x = 1.25 \text{ m}$, and GPU simulations are carried out with grid spacings equal to 1.25, 2.5, 5, 10 and 20 m. The reference distribution of temperature at $t = t_{tot}$ is shown in Fig S3b. Relative deviation of temperature profile at $t = t_{tot}$ from the reference temperature for all grid resolutions is shown

in Fig. S3c. Maximal deviation reaches 7% at the center of the dike and doesn't depend significantly on the grid spacing. That indicates that the main source of deviation is not the spatial resolution, but the solution method. We conclude that the accuracy of the GPU solver is sufficient for making first-order predictions of magma chamber formation.

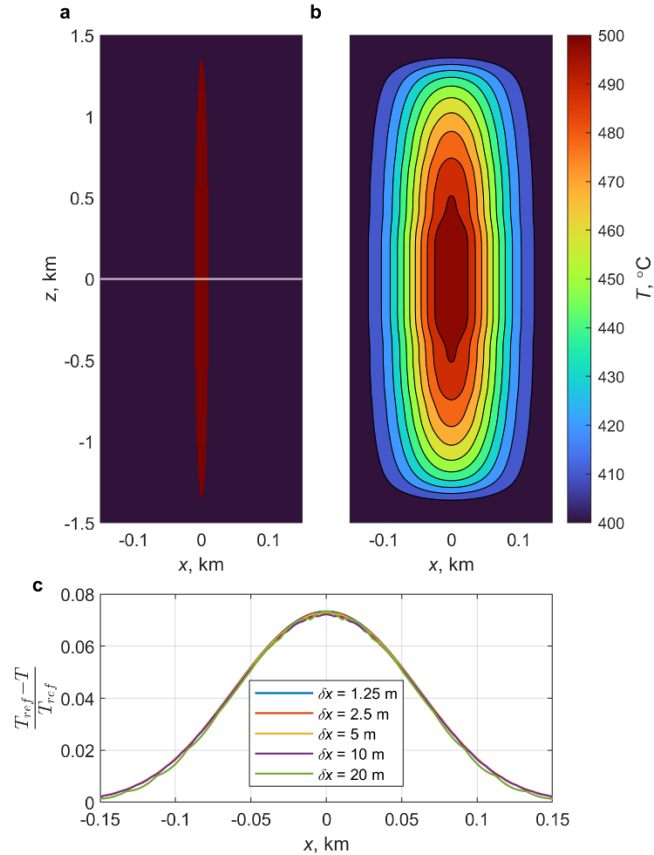


Figure S3. Results of the benchmark study. (a) Problem statement and (b) the deviation of the temperature in the dike computed using enthalpy method and the temperature computed using our explicit GPU code at different grid resolutions.

In the third benchmark study, we compare the results of modelling the repeated injection of rhyolitic dikes into the granitic crust, presented in the main text in the section 3.1, at different grid resolutions, corresponding to grid spacing of 2.5, 5, and 10 m. Characteristic width of a dike is 20 m, and spatial resolution of 10 m is not sufficient for accurate modeling of cooling and solidification, and the results, shown in Fig S4 a and d, are significantly different from other cases, in which the spatial resolution is higher. Distributions of melt fraction at $t = 75$ ky, computed with grid resolutions 5 and 2.5 m, do not differ significantly from each other.

Therefore, we conclude that the grid spacing equal to 5 m is sufficient to resolve the details of the interaction between individual dikes and surrounding rocks.

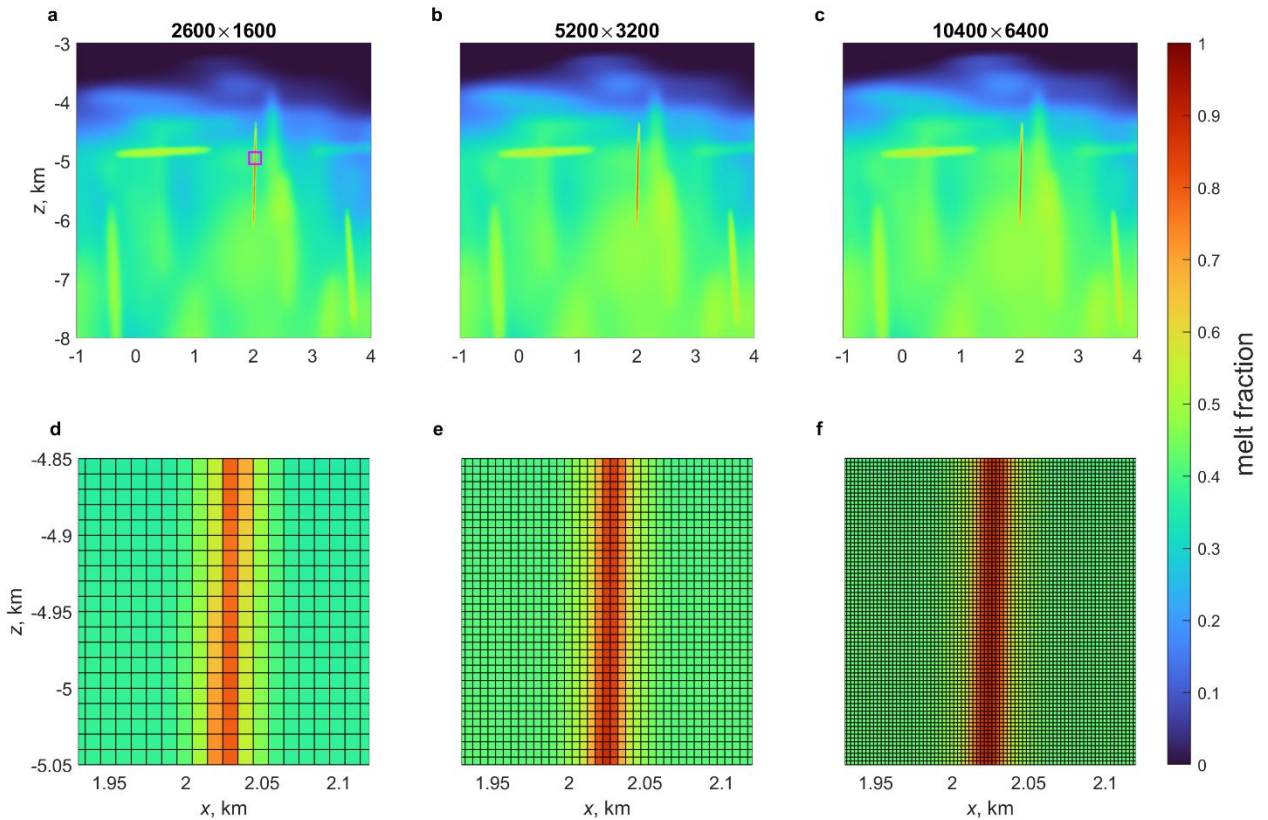


Figure S4. Results of the mesh sensitivity study. In panels the distribution of melt fraction at $t = 75\text{ky}$ is shown. Three columns (a)/(d), (b)/(e), and (c)/(f) correspond to grid resolutions 2600×1600 , 5200×3200 , and 10400×6400 grid points with grid spacing 10 m, 5 m, and 2.5 m, respectively. The first row (a)-(c) is the region of the whole computational domain with coordinates $x \in [-1; 4]$ km and $z \in [-8; -3]$ km; the second row (d)-(f) is the zoomed region of the domain location of which is shown in panel (a) with the magenta rectangle.

Text S2. Enthalpy method, code

```

1 | clear;figure(1);clf;colormap jet
2 | % physics
3 | rho      = 2650;
4 | Cp       = 1350;
5 | L        = 3.5e5;
6 | lambda   = 1.5;
7 | Ly       = 4000;
8 | lam_rhoCp = lambda/rho/Cp;
9 | dT       = 500;
10 | % scales
11 | tsc      = Ly^2/lam_rhoCp;
12 | % nondimensional
13 | Lx_Ly    = 0.25;
14 | L_Cp     = 260;
15 | Ta_dT    = 4/5;
16 | a_Ly     = 0.3375;
17 | b_Ly     = 0.0025;
18 | % dimensionally dependent
19 | Lx       = Lx_Ly*Ly;
20 | a        = a_Ly*Ly;
21 | b        = b_Ly*Ly;

```

```

22 | ttot      = 1e-3*tsc;
23 | Ta        = Ta_dT*dT;
24 | % numerics
25 | ny        = 800;
26 | nx        = ceil(Lx_Ly*ny);
27 | CFL       = 0.1;
28 | niter     = 100;
29 | eiter     = 1e-8;
30 | nout      = 100;
31 | n_lut     = 1001;
32 | % preprocessing
33 | dx        = Lx/(nx-1);
34 | dy        = Ly/(ny-1);
35 | xs        = -Lx/2:dx:Lx/2;
36 | ys        = -Ly/2:dy:Ly/2;
37 | [x,y]     = ndgrid(xs,ys);
38 | dt        = CFL*min(dx,dy)^2/lam_rhoCp;
39 | nt        = ceil(ttot/dt);
40 | dt        = ttot/nt;
41 | % hires numerics
42 | ny_hires  = 6400;
43 | nx_hires  = ceil(Lx_Ly*ny_hires);
44 | % hires preprocessing
45 | dx_hires  = Lx/(nx_hires-1);
46 | dy_hires  = Ly/(ny_hires-1);
47 | xs_hires  = -Lx/2:dx_hires:Lx/2;
48 | ys_hires  = -Ly/2:dy_hires:Ly/2;
49 | [x_hr,y_hr] = ndgrid(xs_hires,ys_hires);
50 | r         = (x_hr/b).^2+(y_hr/a).^2
51 | % init
52 | T0_hr     = Ta*ones(nx_hires,ny_hires);
53 | T0_hr(r<=1) = Ta + dT;
54 | T0        = T0_hr;
55 | for iconv = 1:log2(fix(ny_hires/ny))
56 |     T0 = 0.25*(T0(1:2:end,1:2:end)...
57 |         + T0(2:2:end,1:2:end)...
58 |         + T0(1:2:end,2:2:end)...
59 |         + T0(2:2:end,2:2:end));
60 | end
61 | T_lut     = linspace(300,1000,n_lut);
62 | H_lut     = rho*Cp*T_lut + rho*L*beta_rhyolite(T_lut);
63 | T_itp     = griddedInterpolant(H_lut,T_lut);
64 | H_itp     = griddedInterpolant(T_lut,H_lut);
65 | H         = H_itp(T0);
66 | qx        = zeros(nx+1,ny);
67 | qy        = zeros(nx,ny+1);
68 | % action
69 | for it = 1:nt
70 |     H_old = H;
71 |     errs  = [];
72 |     for iter = 1:niter
73 |         H_err = H;
74 |         T     = T_itp(H);
75 |         qx(2:end-1,:) = -lambda.*diff(T,1,1)/dx;
76 |         qy(:,2:end-1) = -lambda.*diff(T,1,2)/dy;
77 |         divQ      = diff(qx,1,1)/dx + diff(qy,1,2)/dy;
78 |         H         = H_old - dt*divQ;
79 |         H_err     = H_err - H;
80 |         merr      = max(abs(H_err(:)))/max(abs(H(:)));
81 |         if merr < eiter; break; end
82 |     end
83 |     if mod(it,nout) == 0
84 |         pcolor(x,y,T); shading flat; axis image; colorbar; caxis([Ta Ta+dT])

```

```

85     title(sprintf('it = %d, iter = %d',it,iter))
86     drawnow;
87     end
88 end
89 pcolor(x,y,T); shading flat; axis image; colorbar; caxis([Ta Ta+dT])
90 title(sprintf('it = %d, iter = %d',it,iter))
91 function bt=beta_rhyolite(T)
92     T2 = T.*T;
93     t7 = exp(0.961e3 - 0.359e1*T + 0.448e-2*T2 - 0.187e-5*T2.*T);
94     bt = 0.1e1./(0.1e1 + t7);
95 end
96

```

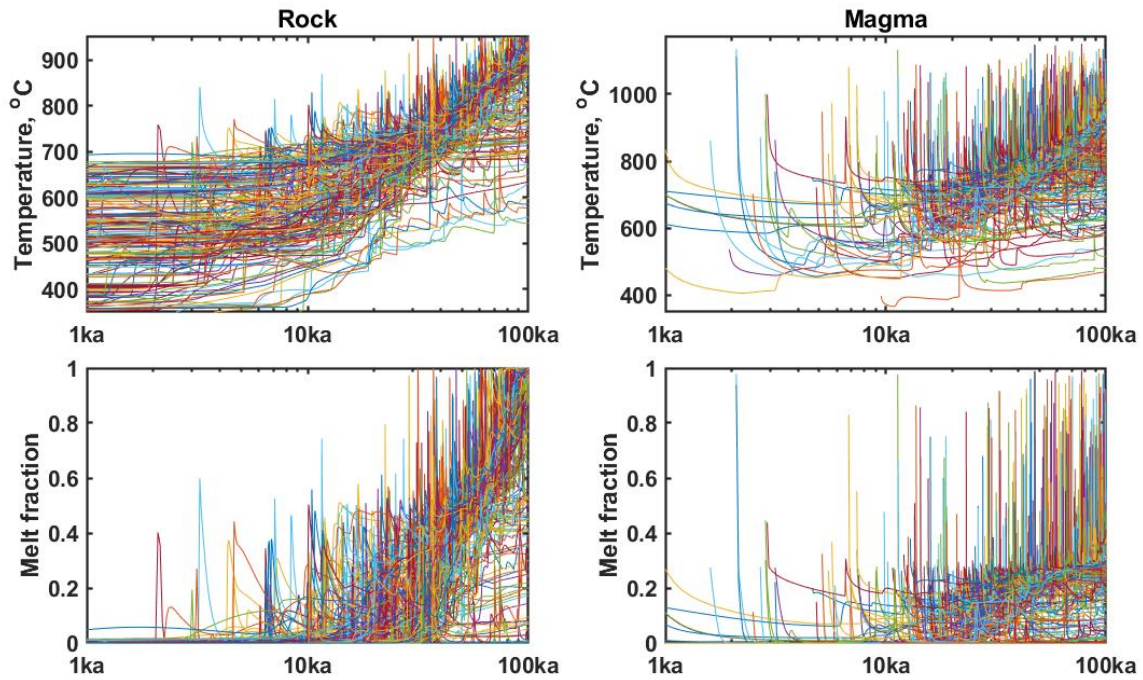


Figure S5. Temperature histories of rock and magma particles during basaltic magma injection into granitic host rocks for $Q=0.25 \text{ m}^3/\text{s}$, $W=10 \text{ km}$. Due to higher solidification temperatures basaltic magma has low melt fraction soon after the emplacement, while host rocks become completely molten.

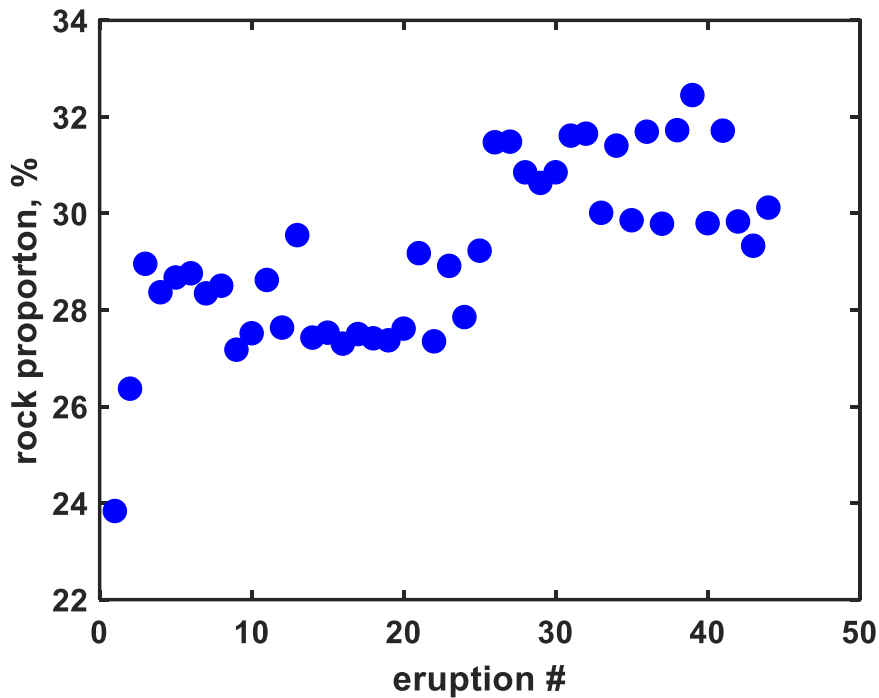


Figure S6. Proportion of assimilated rocks during different eruptions.

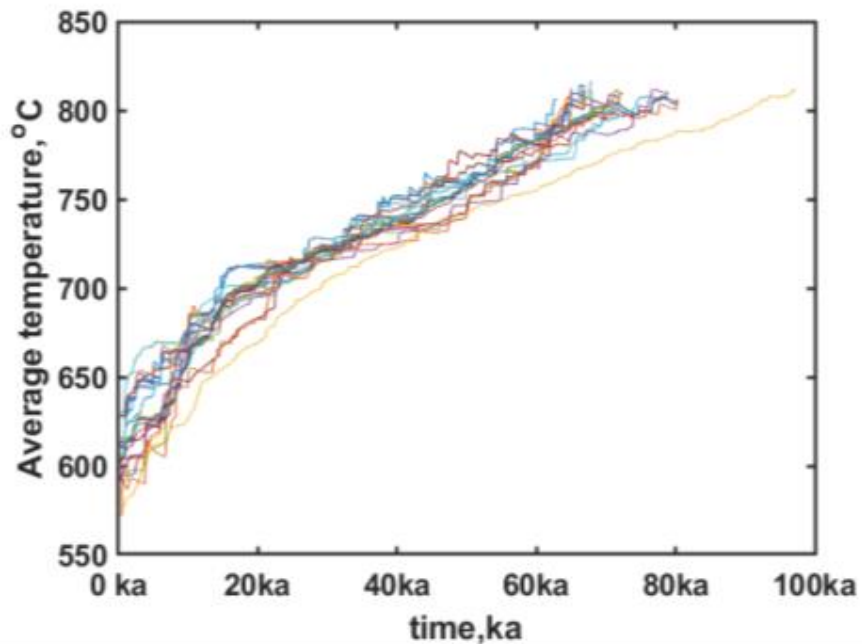


Figure S7. Average temperature of host rocks vs. time during preparation to different eruptions shown on Figs.8-10. Because most eruptions are generated from the bottom of the magma injection area, the starting temperature is ~ 570-620 °C. With consequent injection of new magma and heat transfer the temperature rises to ~ 800 °C, that corresponds to ~ 50 % melt (see Fig. S1)

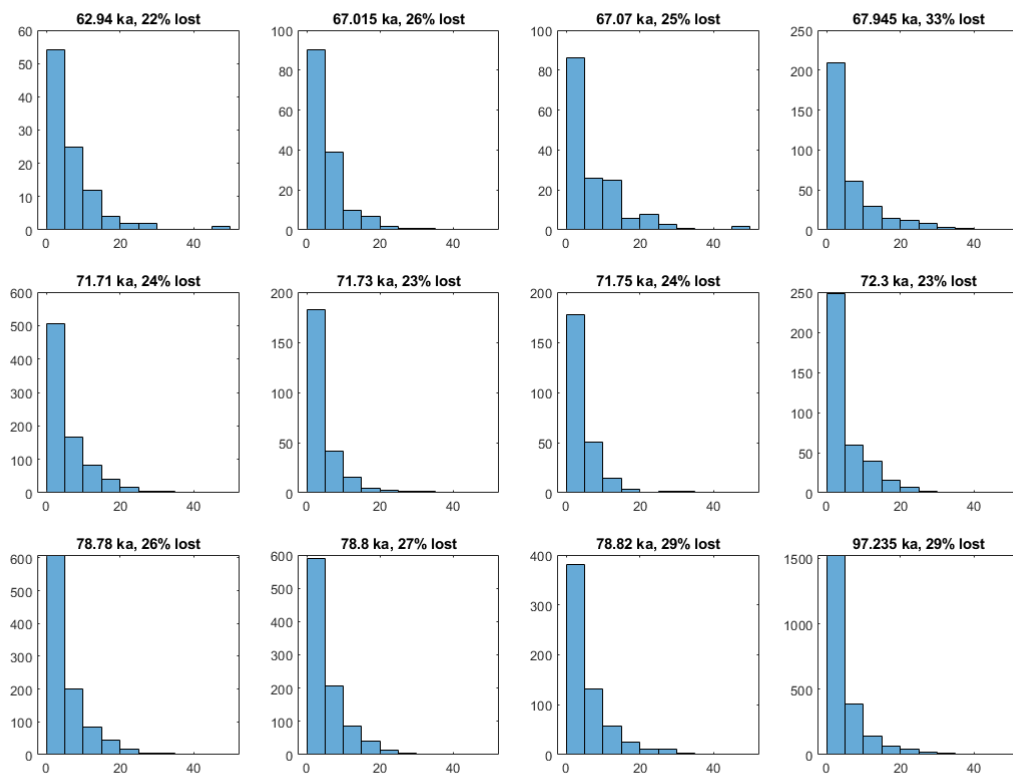


Figure S8. Histograms of core preservation of different host-rock zircon crystals during different eruption episodes.